

Robust multi-objective optimization under multiple-uncertainties using CM-ROPAR approach: case study of the water resources allocation in the Huaihe River Basin

Jitao Zhang^{1,2,3}, Dimitri Solomatine^{2,3,4}, Zengchuan Dong¹

¹College of Hydrology and water resources, Hohai University; Nanjing, 210000, China.

²Water Resources Section, Delft University of Technology; Delft, 2628 CD, Netherlands.

³IHE Delft Institute for Water Education; Delft, 2628 AX, Netherlands

⁴Water Problems Institute of RAS, Moscow 119333, Russia

Correspondence to: Zengchuan Dong (zcdong@hhu.edu.cn)

Abstract. Water resources managers need to make decisions in a constantly changing environment because the data relating to water resources is uncertain and imprecise. The Robust Optimization and Probabilistic Analysis of Robustness (ROPAR) algorithm is a well-suited tool for dealing with uncertainty. Still, the failure to consider multiple uncertainties and multi-objective robustness hinder the application of the ROPAR algorithm to practical problems. This paper proposes a robust optimization and robustness probabilistic analysis method that considers numerous uncertainties and multi-objective robustness for robust water resources allocation under uncertainty. The Copula function is introduced for analyzing the probabilities of different scenarios. The robustness with respect to the two objective functions is analyzed separately, and the Pareto frontier of robustness is generated. The relationship between the robustness with respect to the two objective functions is used to evaluate water resources management strategies. Use of the method is illustrated on a case study of water resources allocation in the Huaihe River Basin. The results demonstrate that the method opens a possibility for water managers to make more informed uncertainty-aware decisions.

1. Introduction

Water resources is a natural resource necessary for human survival (Chen et al., 2017) but also a driving force for social and economic development (Dong and Xu, 2019). Due to the increasing population and rapid growth of economy, a contradiction between the supply and demand of water resources is becoming more acute, water quality problems are becoming more prominent, and water resources have gradually become a bottleneck for socio-economic development (Zhuang et al., 2018). This phenomenon is particularly evident in rapidly urbanizing and vital agricultural and industrial production watersheds (Yang et al., 2017). In this category of watersheds, agricultural and industrial production pose a massive challenge to water resource management (WRM) due to accelerated urbanization and rapid socio-economic development (Sun et al., 2019). River basin managers must consider water sources in an integrated manner and decide how to allocate water resources between different water-using sectors and cities within the basin (Xiong et al., 2020).

Multi-objective optimization (MOO) is an effective method for improving water resources allocation

37 (WRA) schemes (Lu et al., 2017; Abdulbaki et al., 2017). MOO can provide decision-makers with WRA
38 options based on their preferences for objectives, which makes it a well-suited decision-making method
39 for WRM. Ashofteh et al. (2013) constructed a bottom-line-based multi-objective optimization model to
40 calculate WRA schemes. Habibi Davijani et al. (2016) presented a multi-objective optimal allocation
41 model of water resources in arid areas based on maximum socioeconomic benefits. However, WRM is
42 not only a multi-stage and multi-objective problem but also a complex problem involving uncertainties
43 and risk management (Yu and Lu, 2018). WRM departments often need to face decision challenges under
44 uncertain conditions (Hassanzadeh et al., 2016; Ren et al., 2019). Climate change and human activities
45 have led to an increase in uncertainties in rainfall and water demand in the basin and hence to uncertainty
46 in managing water resource systems (Jin et al., 2020; Ma et al., 2020; Zhu et al., 2019). Uncertain factors
47 may lead to the risk of water shortage in the basin, so the existing WRA schemes may not be longer
48 applicable (Keath and Brown, 2009). Therefore, it is important to study WRA under uncertainty.

49 Previously, several methods were introduced to analyze uncertainty in WRM. Scenario building and
50 analysis is regarded as an effective method for considering possible future events and analyzing future
51 uncertainties (Zeng et al., 2019). The fuzzy logic theory is one of the methods to deal with uncertainty,
52 which describes uncertainty by fuzzifying the decision variables (Nikoo et al., 2013). Two-stage
53 stochastic programming (TSP) is also an available planning method in optimization under uncertainty
54 (Li et al., 2020). However, these approaches do not explicitly evaluate the robustness of the WRA options,
55 although they take into account the uncertainties in WRA.

56 Robust multi-objective optimization (RMOO) is an effective method for forming robust WRA schemes.
57 In relation to water, RMOO was actively applied in the field of water supply system (Kapelan et al., 2005;
58 Kapelan et al., 2006). In the last decade, RMOO has been gradually applied to other areas of WRM.
59 Yazdi et al. (2015) and Kang and Lansey (2013) applied robust optimization to design wastewater pipes
60 by considering uncertainties such as climate change, urbanization, and population change. Marchi et al.
61 (2016) formed stormwater harvesting schemes under variable climate conditions using RMOO. It should
62 be pointed out however, that in the mentioned approaches the robustness is often “hidden” into the
63 objective function or constraints and then a common MOO problem is solved that forms a single Pareto
64 front. This is indeed an effective method to create solution set which in a certain sense is robust. However,
65 this approach does not explicitly show the relationship between the solution and the uncertainty variables,
66 which prevents the decision-maker from clearly understanding the impact of uncertainty, which can
67 influence the decision. To answer this limitation, the procedure “Robust Optimization and Probabilistic
68 Analysis of Robustness” (ROPAR) has been developed and presented first in (Solomatine, 2012). The
69 method will generate multiple Pareto fronts, each corresponding to a sample of uncertain variables so
70 that the statistical characteristics of the uncertainty of the solution can be analyzed. The ROPAR has been
71 applied in the design of urban stormwater drainage pipes (Solomatine and Marquez-Calvo, 2019) and for
72 water quality management in water distribution (Marquez Calvo et al., 2019; Quintiliani et al., 2019).

73 To the best of our knowledge, the presented versions of the ROPAR methodology have the following
74 limitations: (1) ROPAR method has not been applied to the field of WRA; (2) ROPAR method only
75 considers the single source of uncertainty: if there are two sources, then the joint probability of these
76 sources needs to be considered; (3) ROPAR method only analyses the variability of one objective under
77 conditions where the other objective function level is fixed. Although the ROPAR method can provide
78 decision-makers with a robust solution under certain conditions, it does not take into account the
79 relationship between the two objective functions.

80

81

82 Based on the above analysis, although the ROPAR method has proven to be suitable for dealing
83 with uncertainty, it still needs improvement. In this study, we propose a Copula-Multi-objective Robust
84 Optimization and Probabilistic Analysis of Robustness (CM-ROPAR) procedure under multiple
85 uncertainties for WRA. The proposed new procedure of the ROPAR-family considers the joint
86 probability distribution of uncertainties (in this case, inflows) and enables decision-makers to check the
87 robustness of the two objective functions separately.

88 The following text is structured as follows. First, the Chapter 2 presents the methodology of the
89 paper. It mainly includes the method of Copula function, the method of CM-ROPAR algorithm, the
90 definition of robustness and the construction of water resources allocation model. Then, the Chapter 3
91 introduces the overview of the study area. Then, the Chapter 4 introduces the application examples of
92 CM-ROPAR algorithm, and this paper is an example of water resources allocation of Huaihe River Basin.
93 Finally, the last Chapter introduces the conclusion of the paper.

94

95 2. Methodology

96 2.1 Method of Copula Function

97 Sklar proposed Copula theory in 1959, in which he decomposed an N-dimensional Joint Distribution
98 Function (JDF) into a Copula function and N Marginal Distribution Functions (MDF), which are not
99 required to be the same distribution for N variables and can be used to describe the correlation between
100 arbitrary variables. Nelsen gave a strict definition of Copula function in 1999 (Nelsen et al., 2008).
101 Copula function is the function that connects the JDF with their respective MDF. Copula functions can
102 be expressed as:

$$103 C_{\theta}(u_1, u_2 \dots u_n) = C_{\theta}[F_1(x_1), F_2(x_2) \dots F_n(x_n)] \quad (1)$$

104 where $x_1, x_2 \dots x_n$ are random vectors, $F_1(x_1), F_2(x_2) \dots F_n(x_n)$ are MDF of the random vectors,
105 θ is the parameter of copula function.

106 The basic copula functions are mainly classified into Archimedean, elliptic, and quadratic types.
107 Among them, Archimedean Copula functions have been widely applied in the field of hydrology. The
108 most used Archimedean Copula multidimensional joint distribution models are the following:

109 (1) GH-Copula joint distribution model

$$110 C_{\theta}(u_1, u_2 \dots u_n) = \exp \left[-(\sum_{i=1}^n (-\ln u_i)^{\theta})^{\frac{1}{\theta}} \right] \quad (\theta > 1), \quad (2)$$

111 (2) Clayton Copula joint distribution model

$$112 C_{\theta}(u_1, u_2 \dots u_n) = \left[1 + \sum_{i=1}^n (u_i^{-\theta} - 1) \right]^{-\frac{1}{\theta}} \quad (\theta > 1), \quad (3)$$

113 (3) Frank Copula joint distribution model

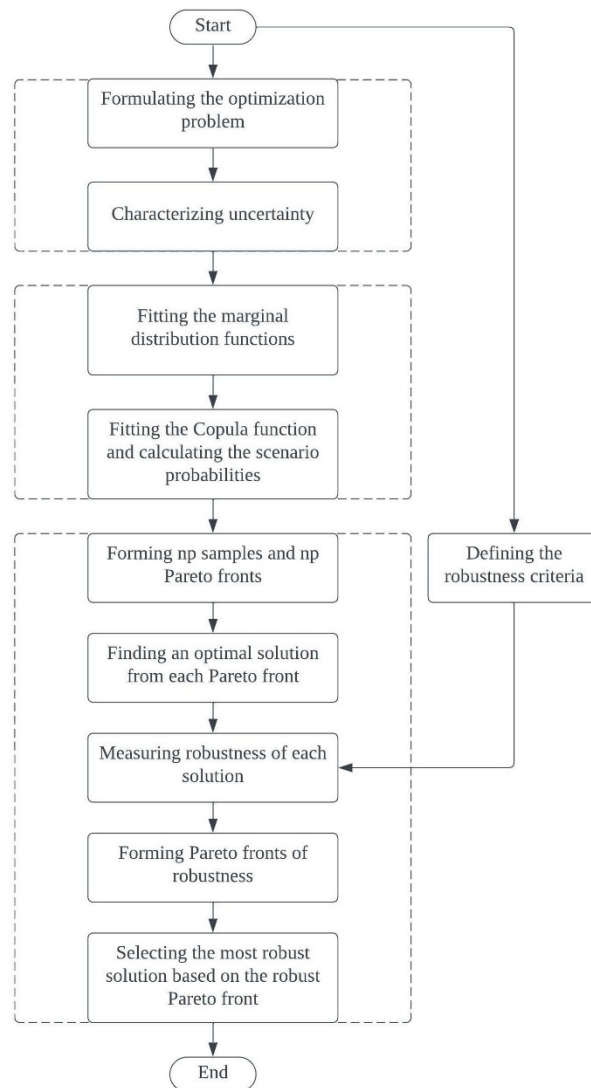
$$114 C_{\theta}(u_1, u_2 \dots u_n) = -\frac{1}{\theta} \ln \left[1 + \frac{\prod_{i=1}^n (e^{-\theta u_i} - 1)}{(e^{-\theta} - 1)^{n-1}} \right] \quad (\theta > 1), \quad (4)$$

115 In a river basin, there may be different drought or wet conditions between different intervals of
116 inflow, so the probability of drought and wet encounters between different intervals of inflow needs to
117 be investigated. According to the analysis in Section 2.1, it is known that Copula function can be used to
118 construct the multivariate joint distribution function. Therefore, this paper adopts Copula function theory

119 to construct the joint distribution and analyze the drought and wet encounter probability. The steps of
 120 Copula function-based wet-dry encounter analysis are as follows: 1. Fit and Select the MDF. The widely
 121 applied probability distribution functions are mainly Pearson type 3 distribution (P-III), T-distribution,
 122 Normal distribution, etc. 2. Fit and Select Copula distribution function. Fitting different MDF of the
 123 runoff, using the AIC and BIC criterion for the selection of the fitted MDF. 3. Calculate the probability
 124 of a dry and wet encounters between different interval inflows.
 125

126 2.2 Method of CM-ROPAR

127 The basic flow of CM-ROPAR algorithm is shown in Figure 1. Firstly, the multi-objective optimization
 128 problem is defined and the uncertainty variables are clarified; secondly, the Copula function is used to
 129 analyze the relationship between the two sources of uncertainty; and finally, through sampling and multi-
 130 objective optimization calculations, the robustness of each solution is identified and the one with the
 131 most comprehensive robustness is selected.
 132
 133



134

135 **Figure 1.** Flowchart of CM-ROPAR.

136

137 The specific process of optimal water allocation under runoff uncertainty based on MROPAR algorithm
138 is as follows.

139 **Part 1** (Analyzing the wet-dry encounters)

140 1. Analyze the inflow wet and dry encounters. If the basin has k inflows, then there are 3^k wet-
141 dry scenarios. For example, suppose there is one inflow in the upper and one in the middle reaches of the
142 basin. In that case, there are 9 scenarios: wet-medium, wet-wet, medium-wet, medium-medium, medium-
143 dry, dry-wet, dry-medium, and dry-dry.

144 2. Choose a scenario from 1 to 3^k .

145 **Part 2** (Sampling-Inflow)

146 3. Based on the recorded annual inflow data Q , it is assumed that Q is not a definite value but

$$147 \quad Q = i_{uncertainty} * Q, \quad (5)$$

$$148 \quad i_{uncertainty} \sim N(\mu, \sigma^2), \quad (6)$$

149 where $i_{uncertainty}$ follows a normal distribution.

150 4. For $i = 1 \dots np$ do

151 5. Sample u (inflow). As mentioned before, the uncertainty variable is obtained from the normal
152 distribution $N(\mu, \sigma^2)$. Assuming that the uncertainty variable follows $N(1, 0.0025)$, this
153 represents that a 99.74% probability of the uncertainty variable falling within the
154 interval $[0.85, 1.15]$ and the inflow sample falling within the interval $[0.85 * Q, 1.15 * Q]$.
155

156 **Part 3** (Forming the optimal solution set through np Pareto fronts)

157 7. Select an ideal solution (IS) in each Pareto front F_r based on the distance to the origin point,
158 forming the optimal solution set (set S).

159 **Part 4** (Evaluate the robustness of each solution)

160 8. Select a solution s_i ($i = 1 \dots np$) from the solution set S .

161 9. Cast the inflow case u_r ($r = 1 \dots np$) into s_i and calculate $P_r(u_r, s_i)$ and $WD_r(u_r, s_i)$,
162 respectively, to form 1200 values of P_r and WD_r ($r = 1 \dots np$).

163 10. Select the robustness evaluation criteria, $RC1, RC2, RC3, RC4$.

164 11. For each s_i ($i = 1 \dots np$), calculate the $RC1, RC2, RC3, RC4$ and SRI corresponding to P_r
165 and WD_r respectively. Plot the corresponding graphs and find the Pareto front of each graph.

166 12. Find the solution with the highest robustness.

167 End

168 2.3 Defining the robustness criteria

169 According to the general definition of robustness, four common Robustness Criteria (RC) were used in
170 this study (Beyer and Sendhoff, 2007). These must be minimized to achieve the maximum robustness of
171 the solution, so the lower the criteria, the higher the robustness.

172 For the four RC , two MOO are implicitly defined, and optimization can be named Two Layer-Multi-
173 objective optimization of Robustness Criteria (TL-MOORC). It is worth noting that TL-MOORC differs
174 from the problem's MOO. A one-layer MOORC is a solution that may not be minimized at all four RC
175 simultaneously. This problem can be solved by aggregating the four RC into one, for example, using a
176 linear weighted combination. The second layer of MOORC is that for the two objective functions of a
177 solution, the RC for both objective functions may not be minimized at the same time. Therefore, a trade-
178 off must be made between the RC for the two objective functions.

179 The first RC is the expected value of each objective function, denoted as $RC1$. It reflects the fact that
 180 we want to find a solution that is good on average across all uncertainties and can be represented by:

$$181 \quad RC1(s) = \int_{N(s,u)} f(s,u) p(u) du, \quad (7)$$

182 Where is the probability density function of the uncertain variable u ; it is the neighborhood of the
 183 solution s .

184 The second RC is the ‘worst case’ (or ‘minimax’ case), denoted as $RC2$. This RC is related to
 185 robustness because we want to find a solution s such that the value of each objective function in the
 186 worst case is the minimum possible. It can be presented as follows:

$$187 \quad RC2(s) = \min \left(\max_{N(s,u)} (f(s,u)) \right), \quad (8)$$

188 The third RC is the ‘standard deviation’ of each objective function, denoted as $RC3$. $RC3$
 189 is related to the robustness of each objective function because we want to find a solution s such that
 190 the value of the objective function would not vary too much due to uncertainty. It can be expressed as
 191 follows:

$$192 \quad RC3(s) = \sqrt{\int_{N(s,u)} (f(s,u) - f(u))^2 p(u) du}, \quad (9)$$

193 The fourth RC is the "probabilistic threshold", denoted as $RC4$. We want to find a solution s that
 194 minimizes the probability that the objective function is higher than the threshold of interest q . This
 195 criterion is usually associated with the reliability of the system. It can be expressed as follows:

$$196 \quad RC4(s) = Pr(f(s,u) > q|s), \quad (10)$$

197 In order to evaluate the integrated robustness of the water resources allocation scheme, the weighted
 198 sum of the four Normalized RC ($NRCi$) in this study was used as the integrated robustness criteria. In
 199 this study, we consider that the four RC to be of equal importance, so all four indicators are given a
 200 weight of $\frac{1}{4}$.

$$201 \quad SRI = \frac{1}{4} NRC1 + \frac{1}{4} NRC2 + \frac{1}{4} NRC3 + \frac{1}{4} NRC4, \quad (11)$$

202 (of course, other ways of aggregation can be considered as well.)

203 2.4 Construction of WRA Model

204 Objective function

205 (1) Social Goals: Water Deficit (WD)

$$206 \quad \min f_1(Q) = \sum_{j=1}^J \sum_{k=1}^K \left(\frac{D_{jk} - \sum_{t=1}^T \sum_{i=1}^I Q_{ijkt}}{D_{jk}} \right)^2, \quad (12)$$

207 Where D_{jk} denotes the water demand of the water consumption department k of the city j . Q_{ijkt} is the
 208 water supply quantity of water source i to water consumption department k of the city j in the period
 209 t .

210 (2) Ecological goals: Pollution (P)

$$211 \quad \min f_2(Q) = \sum_{j=1}^J \sum_{k=1}^K d_{jk} p_{jk} \sum_{i=1}^I \sum_{t=1}^T Q_{ijkt}, \quad (13)$$

212 Where d_{jk} denotes the representative pollutant discharge per unit of wastewater of the water department
 213 k of calculation unit j (ton/m³) and p_{jk} represents the sewage discharge coefficient of the water
 214 consumption department of calculation unit. Discharge coefficient of water consumption department k
 215 of calculation unit j . Q_{ijkt} is the water supply quantity of water source i to water consumption
 216 department k of calculation unit j in the period t .

217 Constraints

218 (1) Water demand constraint

219
$$\sum_{i=1}^I \sum_{t=1}^T Q_{ijkt} \leq D_{jk}, \quad (14)$$

220 (2) Water supply capacity constraint

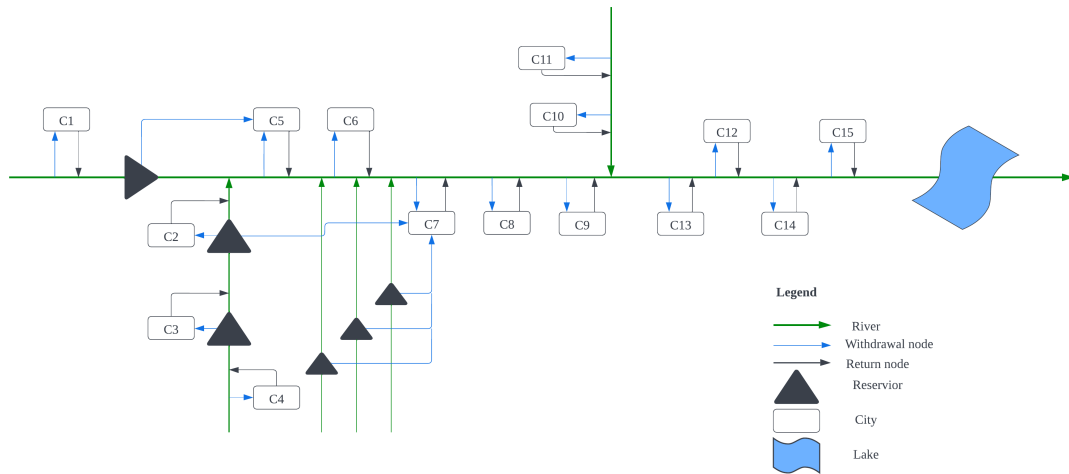
221
$$\sum_{k=1}^K \sum_{j=1}^J \sum_{t=1}^T Q_{ijkt} \leq U_i, \quad (15)$$

222 (3) Water Resources Constraint

223
$$\sum_{j=1}^J \sum_{k=1}^K Q_{ijk} \leq WR_i, \quad (16)$$

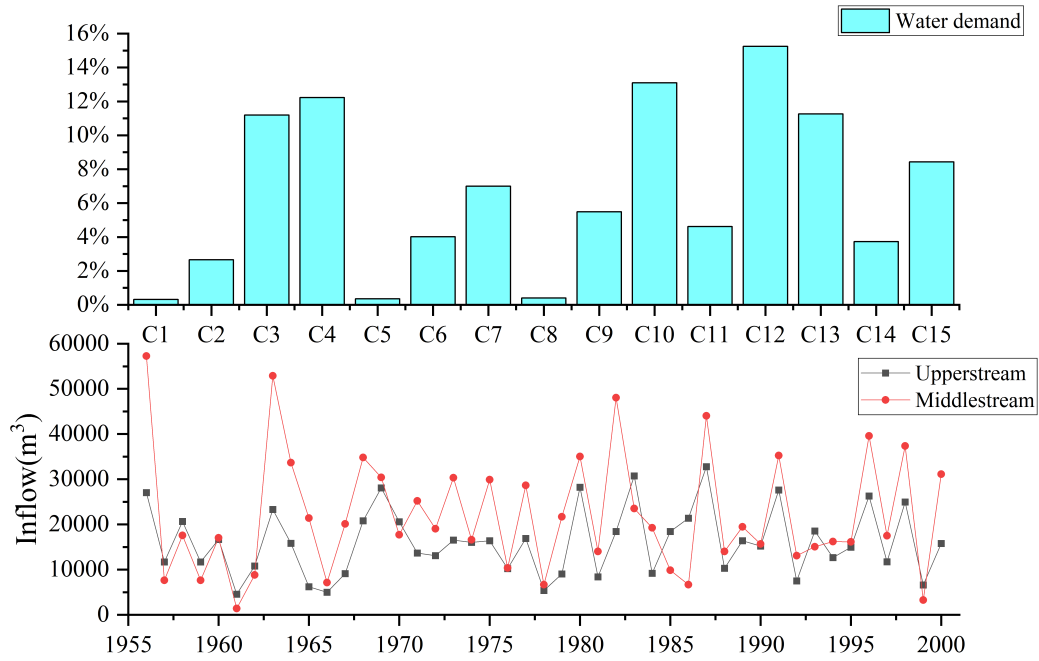
224 3. Study Area Overview

225 The Huaihe River Basin is located in the eastern part of China, and as shown in Figure 2, the middle and
226 upper basin flows through 15 cities of Henan Province and Anhui Province. It is an important agricultural
227 and industrial production base in China (Xu et al., 2019). As shown in the Figure 3, the inflow of the
228 Huaihe River Basin varies significantly between different years and between different regions, and the
229 water demand is uneven among cities. In this study, water demand is calculated by using the quota
230 method commonly used in the field of water resources. In addition, due to the discharge of pollutants,
231 the contradiction between supply and demand of water resources in the middle and upper reaches of the
232 Huaihe River Basin has become increasingly fierce. Therefore, it is meaningful to study the optimal
233 allocation of water resources and propose a robust water resources allocation scheme based on the wet-
234 dry encounters in the Huaihe River Basin.



235

236 **Figure 2.** Overview of watershed water supply.



237

238 **Figure 3.** Water demand proportion and inflow historical data.

239 4. Results and discussion

240 4.1 Identification of marginal distribution functions

241 According to the first part (step 1-2) of the CM-ROPAR process, we need to construct the joint
 242 probability distributions for the upstream and midstream inflow and generate nine inflow scenarios via
 243 the Copula function. Therefore, before constructing the JDF, we need to construct the MDF for the
 244 upstream and midstream inflows respectively. Based on the Kolmogorov-Smirnov (K-S) test results, we
 245 found that the best-fitting distributions for the upstream and midstream were the Weibull and P-III
 246 distributions, respectively.

247 4.2 Analysis of upstream and midstream dry and wet encounters

248 The optimal Copula function is selected by comparing the Akaike information criterion (AIC) and the
 249 Bayesian information criterion (BIC), AIC and BIC values in Table 1. It can be concluded that the joint
 250 distribution function of the upper and middle reaches of the Huaihe River Basin is consistent with the
 251 joint distribution of the Clayton Copula function.

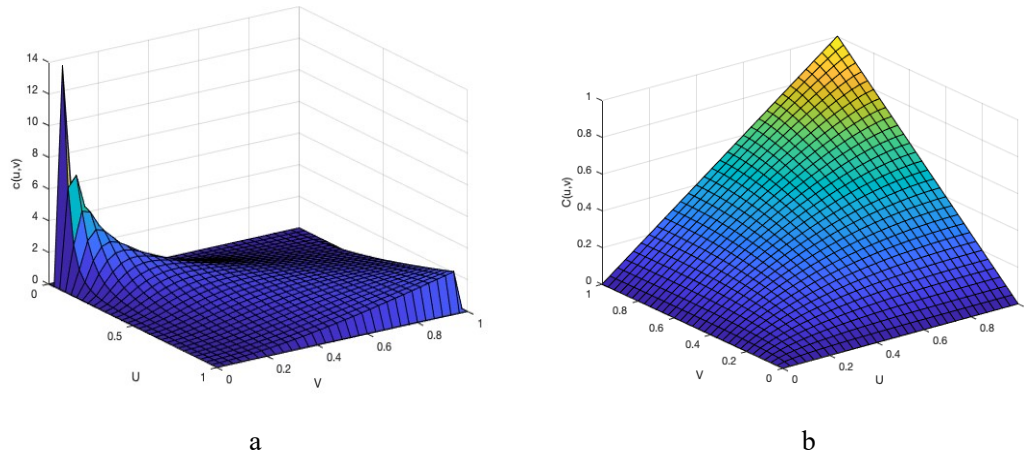
252

253 **Table 1.** AIC and BIC values for Copula functions.

	Gaussian	t	Clayton	Gumbel	Frank
AIC	-20.86	-18.34	-22.69	-12.47	-20.03
BIC	-19.06	-14.73	-20.88	-10.67	-18.22

254

255 Substituting the multi-year annual inflow for the upper and middle reaches of the Huaihe River Basin
 256 into the Clayton Copula function, respectively, the following results were obtained.



257 **Figure 4.** Clayton Copula function.

258
 259 As shown in Figure 4, the joint distribution of the annual incoming water in the upper and middle reaches
 260 of the Huaihe River Basin has symmetry. In addition, the joint distribution of annual water in the upper
 261 and middle reaches has a tail correlation, which indicates a higher probability of simultaneous wetness
 262 or drought in the upper and middle reaches.

263
 264 **Table 2.** The probabilities of 9 scenarios.

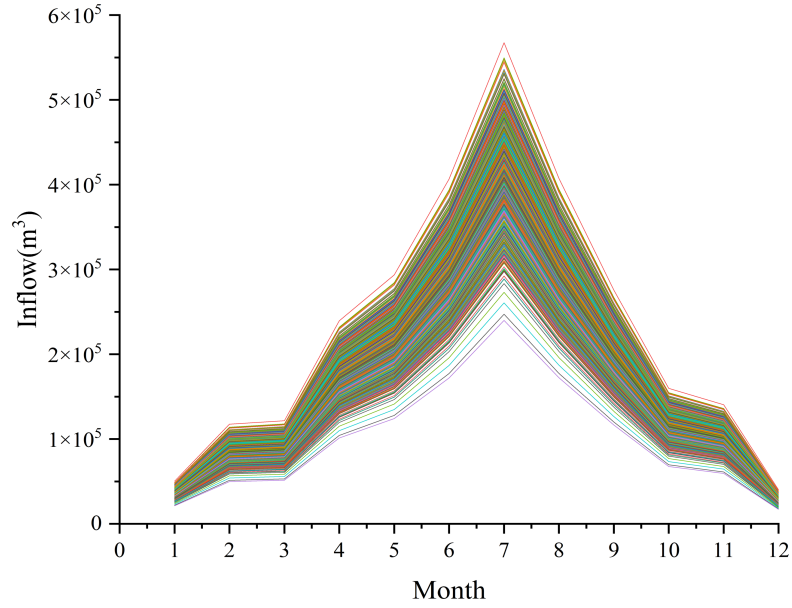
Wet and Dry encounters/%		Upstream		
		Wet	Medium	Dry
Middlestream	Wet	27.7	7.8	5.3
	Medium	11.6	6.5	4.6
	Dry	4.6	7.8	24.1

265
 266 As shown in Table 2, the probability of drought-wetness synchronization in the upper and middle reaches
 267 of the Huaihe River Basin is 58.3%, while the probability of asynchrony is 41.7%. The former is 16.6%
 268 higher than the latter, indicating that the upper and middle reaches are less able to complement each other.
 269 The joint distribution has a maximum probability of 27.7% that the upstream and midstream are both
 270 wet, and the risk of water scarcity is minimal under this scenario. The joint distribution has the second-
 271 highest probability of both upstream and midstream being dry at 24.1%, with the highest risk of water
 272 scarcity under this scenario.

273 4.3 Considering solutions for the uncertainty of inflow through MROPAR

274 In this study the situation when the upper and middle reaches are both wet is considered as a case study.
 275 For deterministic optimization we opted for the NSGA-II algorithm, which is widely used and has good
 276 historical performance (Reed et al., 2013). Inflow uncertainty is modelled by sampling 1200 inflows, as
 277 shown in Figure 5. In this study, NSGA- II algorithm is used for multi-objective function
 278 solving. For algorithm parameterization, the population size is 100, generation is 1000,
 279 cross rate is 0.9 and mutate rate is 0.2.

280

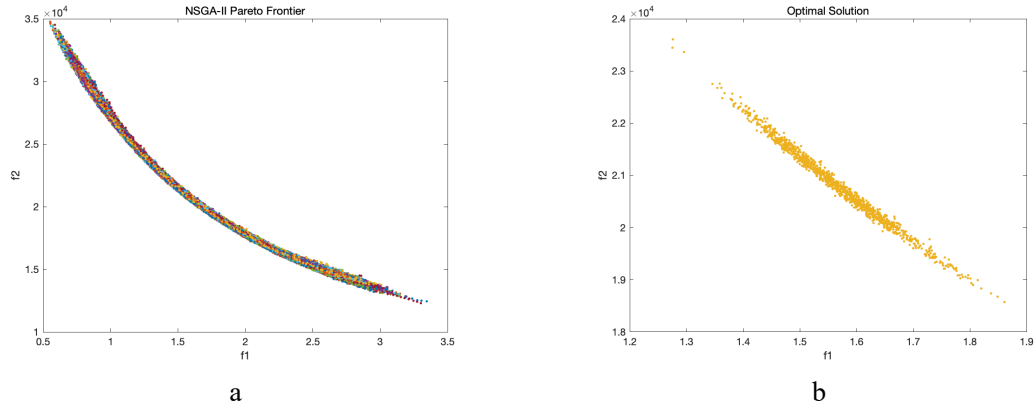


281

282 **Figure 5.** Inflow samples.

283

284 Figure 6(a) shows that 1200 Pareto fronts calculated for each sampled inflow, through steps 3-6 of CM-
 285 ROPAR. Figure 6(b) shows 1200 ideal solutions s , selected based on their distance to the ideal solution
 286 (step 7 of CM-ROPAR).



287

288 **Figure 6.** a: 1200 Pareto fronts (f1: water deficit; f2: pollution) and b: 1200 ideal solutions (f1: water
 288 deficit; f2: pollution) selected based on their distance to the ideal solution.

289

4.4 Assessing robustness of the solutions found by CM-ROPAR

290

291 Four robustness criteria are calculated for each solution s in the solution set S . Given the solution s
 292 to be evaluated, it is necessary to calculate $WD(s, IF_r)(r = 1 \dots np)$ and $P(s, IF_r)(r = 1 \dots np)$ in
 293 order to calculate the four robustness criteria, where IF_r is the $rt\hat{k}$ sample of inflow. r depends on
 294 the number of samples; in this study, 1200 samples were taken, so np is 1200.

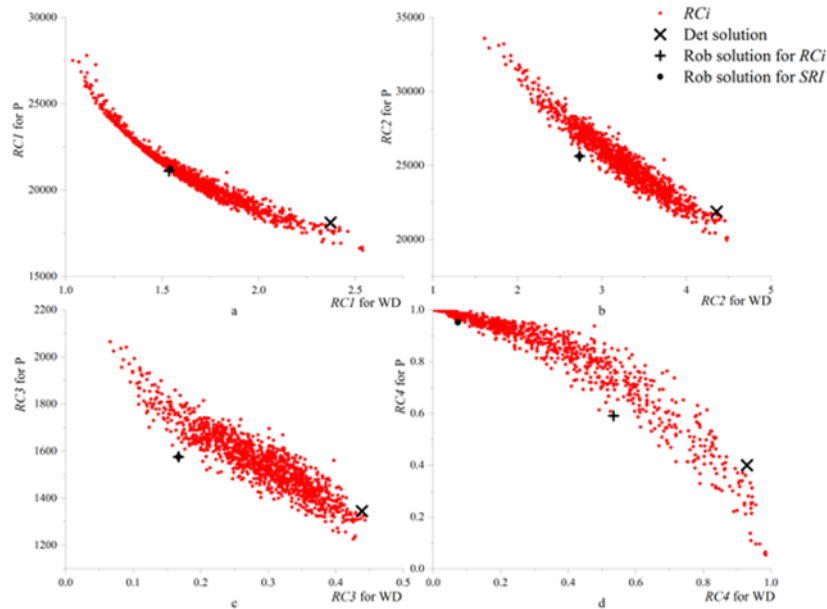
294

295 As shown in Table 3 and Figure 7, $RC1, RC2, RC3, RC4$ and SRI for WD and P can be
 296 calculated for each solution in S , and the solutions corresponding to the smallest value in each RCi and
 297 the solutions corresponding to the smallest value in SRI can be identified, respectively. In addition, we
 298 also feed 1200 samples to the deterministic solution and calculate $RC1, RC2, RC3, RC4$ and SRI for
 299 WD and P .

299

Table 3. Optimal solution numbers for different robustness criteria.

	$RC1$	$RC2$	$RC3$	$RC4$	SRI
WD	535	361	361	361	361
P	876	876	876	876	876
IS	629	84	84	915	84



301

302 **Figure 7.** Performance of the robustness of solutions (a: $RC1$, b: $RC2$, c: $RC3$, d: $RC4$): robust model
 303 solutions (red dots), deterministic model solution (black \times), solution closest to origin for RCi (black +),
 304 solution closest to origin for SRI (black dot). The horizontal axis represents the performance of the
 305 robustness for WD . The vertical axis represents the robustness performance for P .

306

307 Figure 7 shows the performance of 1200 robust model solutions (red dots) and one deterministic model
 308 solution (black \times), for the four robustness criteria. From Figure 7, four Pareto fronts can also be found,
 309 which indicate the competitive relationship between water deficit and pollution emissions for each
 310 robustness criterion dimension. As shown in Figure 7(a), we can observe an interesting phenomenon that
 311 the left-most extreme solution (red dot) has the smallest robustness index $RC1$ for water deficit, but the
 312 highest robustness index $RC1$ for pollution; the right-most extreme solution (red dot) has the largest
 313 robustness index $RC1$ for water deficit, but the smallest robustness index $RC1$ for pollution. Similarly,
 314 this phenomenon can be also observed for the robustness criteria $RC2$, $RC3$, and $RC4$. More
 315 importantly, as shown in Table 3, the extreme solutions and the solutions closest to the origin point may
 316 differ for different robustness criteria. Specifically, for $RC1$, solution No. 535 is the most robust for
 317 water deficit, and solution No. 876 is the most robust for pollution; for $RC2$, $RC3$, and $RC4$, the most
 318 robust solution for water deficit is solution No. 361, and the most robust solution for pollution is solution
 319 No. 876.

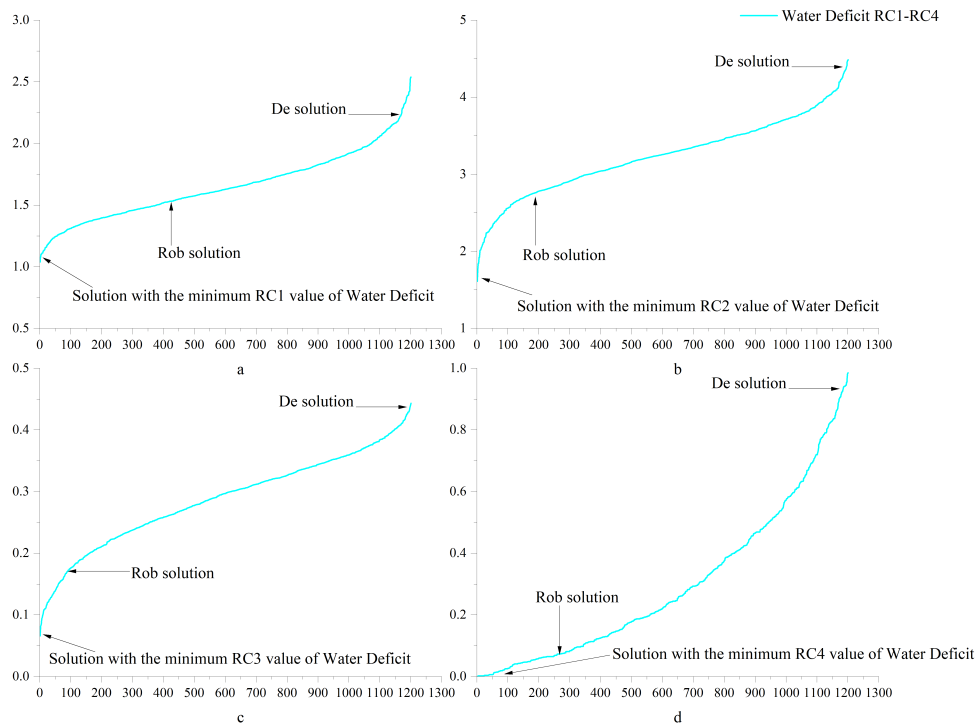
320

Because there are many non-inferior solutions in the Pareto frontier, the decision-makers must
 321 choose among them. The decision-makers need not only to choose among the non-inferior solutions but
 322 also to evaluate the trade-off between different robustness criteria or to choose the best one by combining
 323 the criteria. This study takes the distance to the origin as the basis for such choice. As shown in Table 3,

324 for $RC1$, $RC2$, $RC3$, and $RC4$, the closest points to the origin are solution No. 629, solution No. 84,
 325 and solution No. 915, respectively.

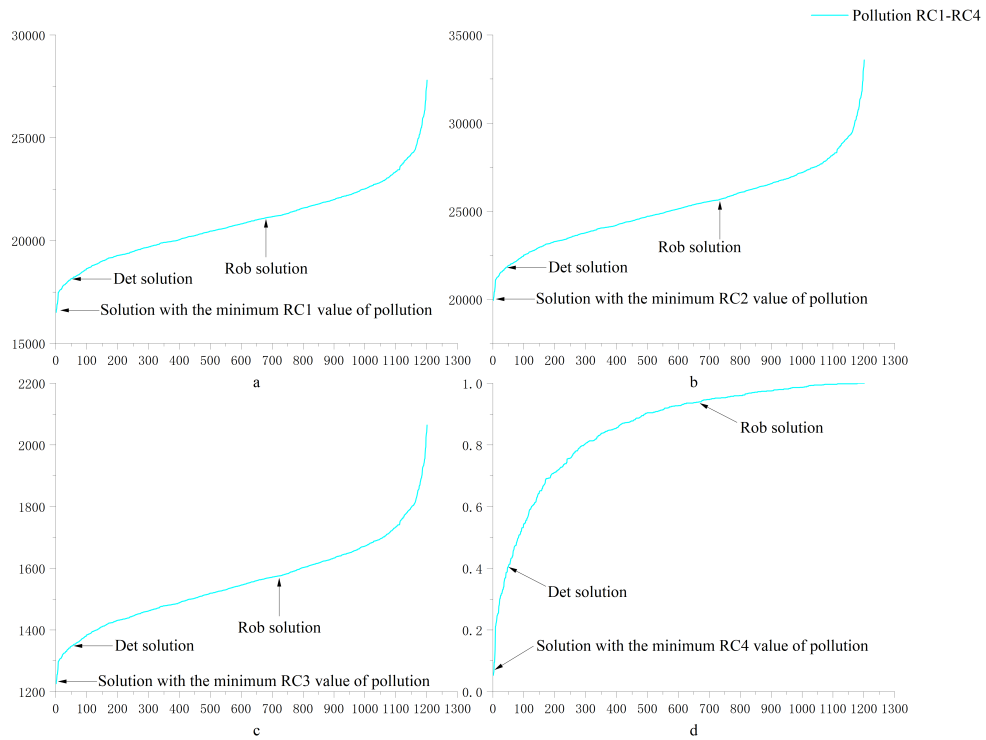
326 **4.5 Comparing solutions found by deterministic and robust approaches**

327 To see a more general relationship between the 1201 solutions (i.e., 1200 from the robust optimization
 328 solution and 1 from the deterministic optimization solution), the performance of each solution for water
 329 deficit and pollution on each of the four robustness criteria (sorted from smallest to largest) is plotted in
 330 Figure 8 and Figure 9.



331 **Figure 8.** Robustness of water deficit (a: $RC1$, b: $RC2$, c: $RC3$, d: $RC4$). The horizontal coordinate
 332 represents the number of solutions and the vertical coordinate represents the robustness of the solution.
 333

334
 335 As shown in Figure 8, for water scarcity, the robust solution performed significantly better than the
 336 deterministic solution. Specifically, for the four robustness criteria, the robust solution outperforms
 337 63.1%, 85.6%, 92.7%, and 77.7% of the solutions, respectively, while the deterministic solution
 338 outperforms only approximately 1% of the solutions. To analyze the robust and deterministic solutions
 339 more accurately and intuitively, this study applied the ratio of $RC(Det)/RC(Rob)$ to compare the
 340 robustness of the two solutions. The ratios of $RC(Det)/RC(Rob)$ are 1.53, 1.59, 2.62, and 12.67 in the
 341 four robustness criteria dimensions. This means that, regarding water deficit, the deterministic model
 342 solution may lead to 53%, 59%, 162%, and 1167% more variability in the four robustness criteria
 343 dimensions.

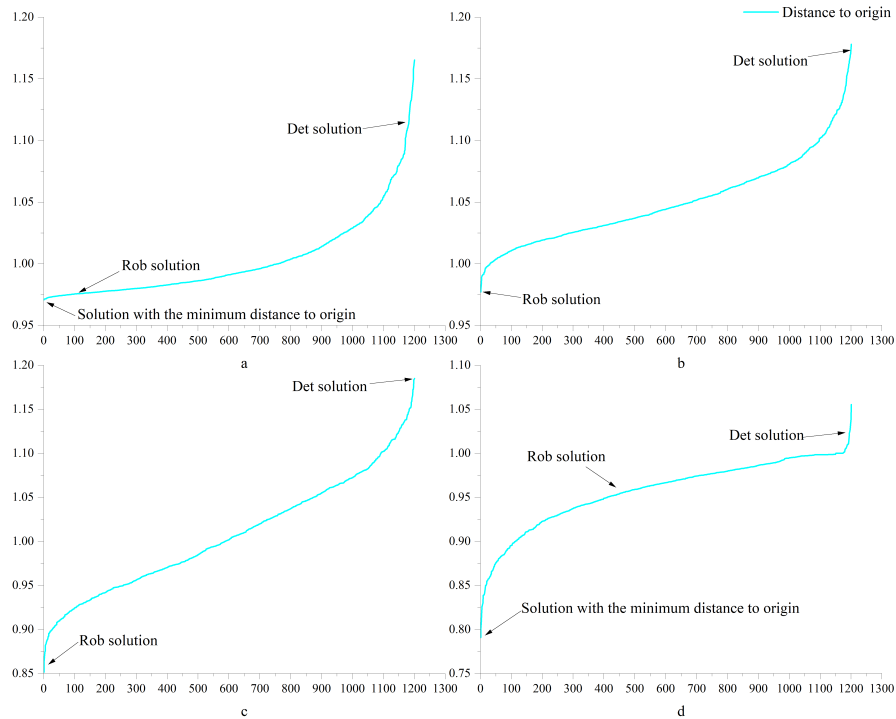


344

345 **Figure 9.** Robustness of pollution (a: $RC1$, b: $RC2$, c: $RC3$, d: $RC4$). The horizontal coordinate
 346 represents the number of solutions and the vertical coordinate represents the robustness of the solution.

347

348 However, as shown in Figure 9, the deterministic solution slightly outperforms the robust solution for
 349 pollution. Specifically, for the four robustness criteria, the deterministic solution outperforms 96% of the
 350 solutions, respectively, while the robust solution outperforms about 40% of the solutions. Similarly, we
 351 compare the two solutions by the ratio of $RC(Rob)/RC(Det)$. We find that the $RC(Rob)/RC(Det)$
 352 ratio is about 1.17 for $RC1$ to $RC3$ and 2.37 for $RC4$. This means that, in terms of pollution, the robust
 353 solution may lead to 17% more variability for $RC1$ to $RC3$ and 137% more variability for $RC4$.

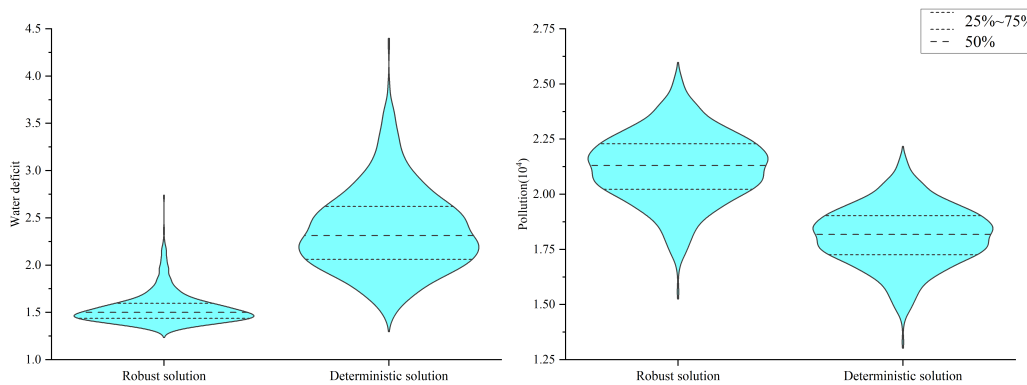


354

355 **Figure 10.** Comprehensive robustness for four indicators (a: $RC1$, b: $RC2$, c: $RC3$, d: $RC4$). The
 356 horizontal coordinate represents the number of solutions and the vertical coordinate represents the
 357 robustness of the solution.

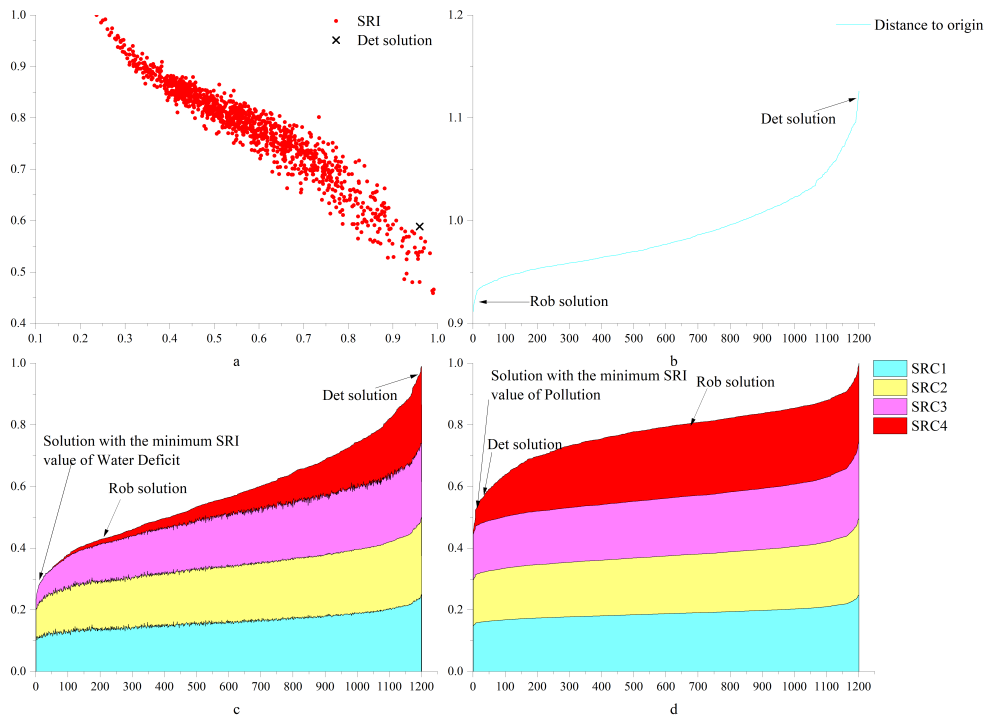
358

359 In order to analyze the comprehensive performance of each solution, rather than just the robustness of a
 360 single objective, this study reflects the comprehensive implementation of each solution in terms of the
 361 distance from the solution to the origin. As shown in Figure 10, the comprehensive performance of the
 362 robust solution for $RC1$ to $RC4$ is significantly better than that of the deterministic model solution.
 363 Specifically, the robust solution outperforms 90.3% and 62.2% of the solutions in $RC1$ and $RC4$,
 364 respectively, and outperforms all solutions in $RC2$ and $RC3$, while the deterministic solution performs
 365 exceptionally poorly in all four robustness criteria. According to the ratio of $Dis(Rob)/Dis(Det)$, we
 366 can find that the robust solution is 16.8%, 19.8%, 39.2%, and 7.3% more robust than the deterministic
 367 solution in the four robustness dimensions, respectively.



368

369 **Figure 11.** The integrated robustness index distribution of the robust and deterministic solution.



370

371 **Figure 12.** Comprehensive robustness criteria performance (a: Performance of comprehensive
 372 robustness criterion, b: Comprehensive robustness of robust solutions and deterministic solution, c and
 373 d: comprehensive robustness criteria for water deficit and pollution).

374

375 As shown in Figure 11, for water scarcity, the integrated criteria of the robust solution is clustered at
 376 approximately 0.5 and is significantly more robust than the deterministic solution; for pollution, the
 377 integrated index of the robust solution is significantly higher than that of the deterministic solution, but
 378 the span of the integrated index of the two solutions is similar, so the robustness of the deterministic
 379 solution is slightly better than that of the robust solution.

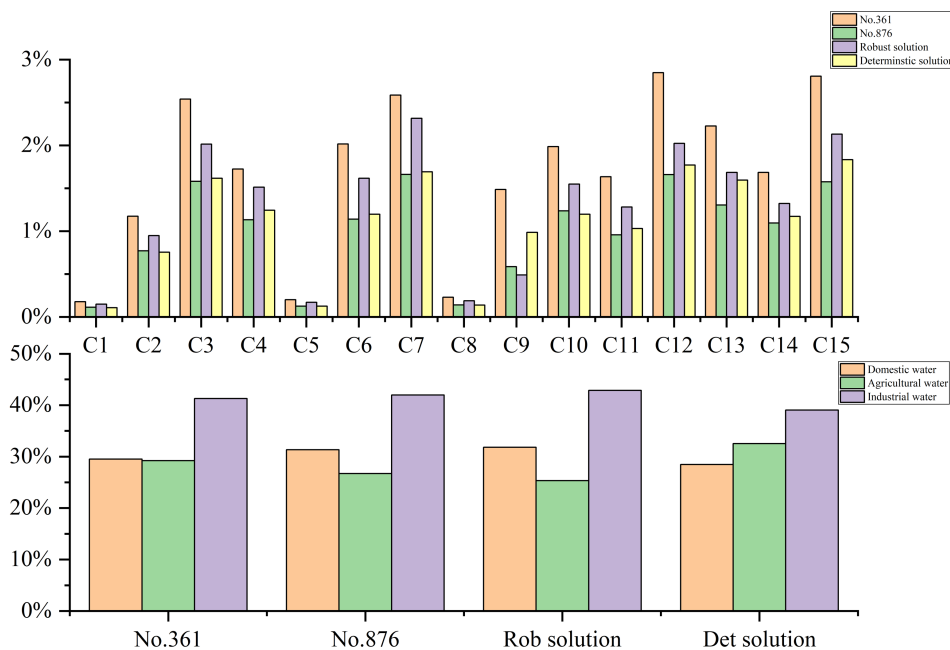
380 Similarly, as shown in Figure 12, there is also a Pareto front for the composite robustness criteria. For
 381 water deficit, the robustness of the robust solution is better than the deterministic solution; for pollution,
 382 the robustness of the deterministic solution is better than the robust solution. Specifically, for water deficit,
 383 the robust solution outperforms 85.3% of the solutions while the deterministic solution outperforms only
 384 about 1% of the solutions; for pollution, the deterministic solution outperforms 96% of the solutions
 385 while the robust solution outperforms only 39.6% of the solutions. According to the ratio of
 386 $SRI(Rob)/SRI(Det)$, the deterministic solution is about 130% more uncertain than the robust solution
 387 for water deficit; for pollution, the robust solution is about 37.7% more variable than the deterministic
 388 solution. The distance of each solution to the origin can reflect the comprehensive performance of the
 389 robustness of each solution. For the robustness composite index, the ratio of $Dis(Rob)/Dis(Det)$ is
 390 0.655, which means that the composite robustness of the robust solution is 52.6% higher than the
 391 robustness of the deterministic solution.

392 For the robustness composite, the robust solution outperforms all the solutions, while the deterministic
 393 model solution outperforms only about 3.2% of the solutions. Comparing the distance to the origin of
 394 the robust solution and the deterministic solution, we can find that the robustness of the robust solution
 395 improves by 27.8% over the deterministic solution.

396 **4.6 Analysis of specific water resources allocation schemes**

397 First, as shown in Figure 13, we analyzed the proportion of water supply for each city. We find that the
 398 water supply share for the scheme most robust to water deficit rates is significantly higher than that for
 399 the scheme with the most robust pollutant emissions. This is because an increase in water supply leads
 400 to an increase in pollutant emissions, which in turn leads to a decrease in the robustness of pollutant
 401 emissions. For specific cities, the least robust allocation scenario for water deficit reduces the water
 402 supply in City 3, City 7, City 10, City 12, and City 15 compared to the most robust allocation scenario
 403 for pollutant emissions. Interestingly, these cities have the most water demand in the basin (as shown in
 404 Figure 3). Therefore, basin managers can increase the water supply to these cities if they need to improve
 405 the water deficit robustness of the water resources allocation scheme.

406 Then we analyze specifically the distribution of water resources between sectors. An interesting
 407 phenomenon can be observed. As shown in Figure 13, although the scenario with the best robustness in
 408 terms of pollutant emissions has a lower water supply than the scenario with the best robustness in terms
 409 of water deficit, the reduction is mainly in the agricultural sector. Water for domestic and industrial
 410 production did not change much. The reason for this may be that agricultural water use causes more
 411 pollution and may create more uncertainty. So how can watershed managers hope that improving the
 412 robustness of pollutant discharge can reduce water supply to the agricultural sector.



413
 414 **Figure 13.** Specific water resources allocation schemes.

415 **5. Conclusion**

416 In this study, we propose a multi-objective robustness analysis method considering multiple uncertainties
 417 (CM-ROPAR approach) based on the robust optimization method for uncertainty perception (ROPAR
 418 approach). To verify the superiority and practicality of the CM-ROPAR approach, four robustness criteria
 419 are selected, and we compare the robust solution calculated by the method with the optimal solution of
 420 the deterministic model. In the studied case, there is a competitive relationship between the robustness
 421 of the two objective functions, which can form a Pareto frontier. For the water deficit rate, the robust
 422 solution outperforms the deterministic solution by 53%, 59%, 162%, and 1167% for the four robustness
 423 criteria, respectively; for the pollutant emission, the deterministic solution outperforms the robust

424 solution by only 17% for *RC1 – RC3*, and outperforms the robust solution by 137% for *RC4*. For the
425 composite robustness, the robust solution outperforms the deterministic solution by 52.6%, the CM-
426 ROPAR finds a more robust solution.

427 The CM-ROPAR approach permits to exhibit the handling of uncertainty, to be able to analyze how
428 uncertainty is transmitted to the Pareto frontier, and to perform the corresponding probabilistic analysis.
429 The novelty of the new method compared to existing ROPAR methods is reflected in two aspects. First,
430 the ROPAR method only considers uncertainty at a single point. In contrast, the CM-ROPAR method
431 considers multiple uncertainties through the joint probability distribution of two points, which is closer
432 to the actual situation and more general. Second, the new way analyzes the robustness of two objective
433 functions of the solution instead of fixing one objective function to analyze the robustness of the other
434 objective function. The CM-ROPAR method is more comprehensive and can identify the robustness of
435 both objective functions, giving decision-makers more information for decision making.

436 One of the limitations of this study is that the CM-ROPAR approach is applicable to problems with
437 two uncertainties and two objective functions; however, water allocation allows for more uncertainties
438 and more objective functions (e.g., the uncertainty of inflow between multiple tributaries). In future
439 research, we will focus on more complex objective functions and multi-objective optimization problems
440 with at least three objective functions.

441

442 *Author contribution.* JZ and DS conceptualized the study and wrote the paper. ZD provided the data. All
443 the authors took part in the interpretation of the results and edits of the paper.

444

445 *Competing interests.* The authors declare that they have no conflict of interest.

446

447 *Acknowledgements.* This research has been supported by the

448

449 **Reference**

450 Abdalbaki, D., Al-Hindi, M., Yassine, A., and Abou Najm, M.: An optimization model for the allocation
451 of water resources, *Journal of Cleaner Production*, 164, 994-1006, 10.1016/j.jclepro.2017.07.024, 2017.

452 Ashofteh, P. S., Haddad, O. B., and A. Mariño, M.: Climate Change Impact on Reservoir Performance
453 Indexes in Agricultural Water Supply, *Journal of Irrigation and Drainage Engineering*, 139, 85-97,
454 10.1061/(asce)ir.1943-4774.0000496, 2013.

455 Beyer, H.-G. and Sendhoff, B.: Robust optimization – A comprehensive survey, *Computer Methods in
456 Applied Mechanics and Engineering*, 196, 3190-3218, 10.1016/j.cma.2007.03.003, 2007.

457 Chen, L., Xu, L., and Yang, Z.: Accounting carbon emission changes under regional industrial transfer
458 in an urban agglomeration in China's Pearl River Delta, *Journal of Cleaner Production*, 167, 110-119,
459 10.1016/j.jclepro.2017.08.041, 2017.

460 Dong, Y. and Xu, L.: Aggregate risk of reactive nitrogen under anthropogenic disturbance in the Pearl
461 River Delta urban agglomeration, *Journal of Cleaner Production*, 211, 490-502,
462 10.1016/j.jclepro.2018.11.194, 2019.

463 Habibi Davijani, M., Banihabib, M. E., Nadjafzadeh Anvar, A., and Hashemi, S. R.: Multi-Objective
464 Optimization Model for the Allocation of Water Resources in Arid Regions Based on the Maximization
465 of Socioeconomic Efficiency, *Water Resources Management*, 30, 927-946, 10.1007/s11269-015-1200-y,
466 2016.

467 Hassanzadeh, E., Elshorbagy, A., Wheeler, H., and Gober, P.: A risk-based framework for water resource

468 management under changing water availability, policy options, and irrigation expansion, *Advances in*
469 *Water Resources*, 94, 291-306, 10.1016/j.advwatres.2016.05.018, 2016.

470 Jin, S. W., Li, Y. P., Yu, L., Suo, C., and Zhang, K.: Multidivisional planning model for energy, water and
471 environment considering synergies, trade-offs and uncertainty, *Journal of Cleaner Production*, 259,
472 10.1016/j.jclepro.2020.121070, 2020.

473 Kang, D. and Lansey, K.: Scenario-Based Robust Optimization of Regional Water and Wastewater
474 Infrastructure, *Journal of Water Resources Planning and Management*, 139, 325-338,
475 10.1061/(asce)wr.1943-5452.0000236, 2013.

476 Kapelan, Z., Savic, D. A., Walters, G. A., and Babayan, A. V.: Risk- and robustness-based solutions to a
477 multi-objective water distribution system rehabilitation problem under uncertainty, *Water Sci Technol*,
478 53, 61-75, 10.2166/wst.2006.008, 2006.

479 Kapelan, Z. S., Savic, D. A., and Walters, G. A.: Multiobjective design of water distribution systems
480 under uncertainty, *Water Resources Research*, 41, 10.1029/2004wr003787, 2005.

481 Keath, N. A. and Brown, R. R.: Extreme events: being prepared for the pitfalls with progressing
482 sustainable urban water management, *Water Sci Technol*, 59, 1271-1280, 10.2166/wst.2009.136, 2009.

483 Li, M., Fu, Q., Singh, V. P., Liu, D., and Gong, X.: Risk-based agricultural water allocation under multiple
484 uncertainties, *Agricultural Water Management*, 233, 10.1016/j.agwat.2020.106105, 2020.

485 Lu, H., Ren, L., Chen, Y., Tian, P., and Liu, J.: A cloud model based multi-attribute decision making
486 approach for selection and evaluation of groundwater management schemes, *Journal of Hydrology*, 555,
487 881-893, 10.1016/j.jhydrol.2017.10.009, 2017.

488 Ma, Y., Li, Y. P., and Huang, G. H.: A bi-level chance-constrained programming method for quantifying
489 the effectiveness of water-trading to water-food-ecology nexus in Amu Darya River basin of Central Asia,
490 *Environ Res*, 183, 109229, 10.1016/j.envres.2020.109229, 2020.

491 Marchi, A., Dandy, G. C., and Maier, H. R.: Integrated Approach for Optimizing the Design of Aquifer
492 Storage and Recovery Stormwater Harvesting Schemes Accounting for Externalities and Climate Change,
493 *Journal of Water Resources Planning and Management*, 142, 10.1061/(asce)wr.1943-5452.0000628,
494 2016.

495 Marquez Calvo, O. O., Quintiliani, C., Alfonso, L., Di Cristo, C., Leopardi, A., Solomatine, D., and de
496 Marinis, G.: Robust optimization of valve management to improve water quality in WDNs under demand
497 uncertainty, *Urban Water Journal*, 15, 943-952, 10.1080/1573062x.2019.1595673, 2019.

498 Nelsen, R. B., Quesada-Molina, J. J., Rodríguez-Lallena, J. A., and Úbeda-Flores, M.: On the
499 construction of copulas and quasi-copulas with given diagonal sections, *Insurance: Mathematics and*
500 *Economics*, 42, 473-483, 10.1016/j.insmatheco.2006.11.011, 2008.

501 Nikoo, M. R., Kerachian, R., Karimi, A., and Azadnia, A. A.: Optimal water and waste-load allocations
502 in rivers using a fuzzy transformation technique: a case study, *Environ Monit Assess*, 185, 2483-2502,
503 10.1007/s10661-012-2726-6, 2013.

504 Quintiliani, C., Marquez-Calvo, O., Alfonso, L., Di Cristo, C., Leopardi, A., Solomatine, D. P., and de
505 Marinis, G.: Multiobjective Valve Management Optimization Formulations for Water Quality
506 Enhancement in Water Distribution Networks, *Journal of Water Resources Planning and Management*,
507 145, 10.1061/(asce)wr.1943-5452.0001133, 2019.

508 Reed, P. M., Hadka, D., Herman, J. D., Kasprzyk, J. R., and Kollat, J. B.: Evolutionary multiobjective
509 optimization in water resources: The past, present, and future, *Advances in Water Resources*, 51, 438-
510 456, 10.1016/j.advwatres.2012.01.005, 2013.

511 Ren, C., Li, Z., and Zhang, H.: Integrated multi-objective stochastic fuzzy programming and AHP

512 method for agricultural water and land optimization allocation under multiple uncertainties, *Journal of*
513 *Cleaner Production*, 210, 12-24, 10.1016/j.jclepro.2018.10.348, 2019.

514 Solomatine, D.: An approach to multi-objective robust optimization allowing for explicit analysis of
515 robustness, <https://www.un-ihe.org/sites/default/files/solomatine-ropar.pdf>, 2012.

516 Solomatine, D. P. and Marquez-Calvo, O. O.: Approach to robust multi-objective optimization and
517 probabilistic analysis: the ROPAR algorithm, *Journal of Hydroinformatics*, 21, 427-440,
518 10.2166/hydro.2019.095, 2019.

519 Sun, S., Fu, G., Bao, C., and Fang, C.: Identifying hydro-climatic and socioeconomic forces of water
520 scarcity through structural decomposition analysis: A case study of Beijing city, *Sci Total Environ*, 687,
521 590-600, 10.1016/j.scitotenv.2019.06.143, 2019.

522 Xiong, W., Li, Y., Pfister, S., Zhang, W., Wang, C., and Wang, P.: Improving water ecosystem
523 sustainability of urban water system by management strategies optimization, *J Environ Manage*, 254,
524 109766, 10.1016/j.jenvman.2019.109766, 2020.

525 Xu, Z., Pan, B., Han, M., Zhu, J., and Tian, L.: Spatial-temporal distribution of rainfall erosivity, erosivity
526 density and correlation with El Niño-Southern Oscillation in the Huaihe River Basin, China, *Ecological*
527 *Informatics*, 52, 14-25, 10.1016/j.ecoinf.2019.04.004, 2019.

528 Yang, W., Li, X., Sun, T., Pei, J., and Li, M.: Macrobenthos functional groups as indicators of ecological
529 restoration in the northern part of China's Yellow River Delta Wetlands, *Ecological Indicators*, 82, 381-
530 391, 10.1016/j.ecolind.2017.06.057, 2017.

531 Yazdi, J., Lee, E. H., and Kim, J. H.: Stochastic Multiobjective Optimization Model for Urban Drainage
532 Network Rehabilitation, *Journal of Water Resources Planning and Management*, 141,
533 10.1061/(asce)wr.1943-5452.0000491, 2015.

534 Yu, S. and Lu, H.: An integrated model of water resources optimization allocation based on projection
535 pursuit model – Grey wolf optimization method in a transboundary river basin, *Journal of Hydrology*,
536 559, 156-165, 10.1016/j.jhydrol.2018.02.033, 2018.

537 Zeng, X., Zhao, J., Wang, D., Kong, X., Zhu, Y., Liu, Z., Dai, W., and Huang, G.: Scenario analysis of a
538 sustainable water-food nexus optimization with consideration of population-economy regulation in
539 Beijing-Tianjin-Hebei region, *Journal of Cleaner Production*, 228, 927-940,
540 10.1016/j.jclepro.2019.04.319, 2019.

541 Zhu, F., Zhong, P.-a., Cao, Q., Chen, J., Sun, Y., and Fu, J.: A stochastic multi-criteria decision making
542 framework for robust water resources management under uncertainty, *Journal of Hydrology*, 576, 287-
543 298, 10.1016/j.jhydrol.2019.06.049, 2019.

544 Zhuang, X. W., Li, Y. P., Nie, S., Fan, Y. R., and Huang, G. H.: Analyzing climate change impacts on
545 water resources under uncertainty using an integrated simulation-optimization approach, *Journal of*
546 *Hydrology*, 556, 523-538, 10.1016/j.jhydrol.2017.11.016, 2018.

547